

BeppoSAX observations of AM Herculis in intermediate and high states

G. Matt¹, D. de Martino², B.T. Gänsicke³, I. Negueruela⁴, R. Silvotti², J.M. Bonnet-Bidaud⁵, M. Mouchet^{6,7}, and K. Mukai⁸

¹ Dipartimento di Fisica, Università degli Studi “Roma Tre”, Via della Vasca Navale 84, I-00146 Roma, Italy

² Osservatorio Astronomico di Capodimonte, Via Moiariello 16, I-80131 Napoli, Italy

³ Universitätssternwarte Göttingen, Geismarlandstrasse 11, D-37083 Göttingen, Germany

⁴ SAX/SDC Nuova Telespazio, Via Corolle 19, I-00131 Roma, Italy

⁵ CEA, DSN/DAPNIA/Service d’Astrophysique, CEN Saclay, F-91191 Gif sur Yvette Cedex, France

⁶ DAEC, Observatoire de Paris, Section de Meudon, F-92195 Meudon Cedex, France

⁷ Université Denis Diderot, 2 Place Jussieu, F-75005 Paris, France

⁸ NASA/GSFC, Code 668, Greenbelt MD 20771, USA

Received 3 January 2000 / Accepted

Abstract. Temporal and spectral analyses from BeppoSAX observations of AM Her performed during both an intermediate and a high state are presented and discussed. Optical observations taken a few days after the X-ray ones are also presented.

During the intermediate state observation, the source was in its “normal”, one-pole accretion mode. In the high state it switched to an hitherto unobserved atypical “two-pole” accretion mode, with significant soft and hard X-ray emission from both poles. The emission from the second pole is much softer than that from the primary pole, while the soft X-ray excess of the primary pole is fairly modest in this accretion mode. These facts suggest that accretion onto the secondary is mainly due to blobs penetrating deeply in the photosphere, while that on the primary pole is mostly via a more homogeneous column, giving rise to the classical standing shock. A strong X-ray flaring activity is also observed in the soft X-ray band, but not the hard X-ray and optical emissions indicating that flares are due to inhomogeneous blobby-accretion events.

Key words: Stars: binaries: close – Stars: cataclysmic variables – X-rays: stars – Stars: individual: AM Herculis

1. Introduction

Polars, a subgroup of magnetic Cataclysmic Variables (mCVs), contain a highly magnetized white dwarf with polar field strengths ranging from ~ 10 MG \sim to 230 MG

Send offprint requests to: G. Matt, matt@fis.uniroma3.it

(see Beuermann 1998 and references therein), and which accretes from a late-type main sequence star. The magnetic field of the white dwarf is strong enough to phase-lock its rotation with the orbital period. These systems are strong X-ray emitters in both soft and hard X-ray bands (see review by Cropper 1990). While hard X-rays and optical cyclotron radiation are emitted from a standing shock above the white dwarf surface, soft X-rays originate from hot photospheric regions heated either by irradiation from the post-shock plasma (Lamb & Masters 1979) or by dense plasma blobs carrying their kinetic energy deep into the atmosphere (Kuipers & Pringle 1982). Irradiation is important primarily for flow rates sufficiently low for the shock to stand high above the surface. However, a large fraction of the reprocessed radiation appears in the UV rather than at soft X-rays, as shown quantitatively in the prototypical system AM Her (Gänsicke et al. 1995).

While the soft X-ray component is in general adequately fitted by a black-body spectrum with a temperature of a few tens of eV (even if more sophisticated models are sometimes needed: see e.g. Van Teeseling et al. 1994), it has recently become clear that a simple thermal plasma model is no longer adequate in reproducing the hard X-ray emission of Polars. Reflection from the white dwarf surface, complex absorption and multi-temperature emission may contribute significantly to the spectrum above a few tenths of keV (e.g. Cropper et al. 1998 and references therein).

Polars are known to display long-term luminosity variations on several timescales ranging from tens of days to years. These variations are thought to be related to changes in the mass transfer rate from the secondary star. The best studied example is again the brightest po-

lar AM Her (Copper 1990; Gänsicke et al. 1995). Such changes come along with spectral variations in all energy bands, indicating changes not only in the spectral parameters of the primary radiation but also in the reprocessed emission. The relative proportion of hard and soft X-ray emissions is expected to be sensitive to the actual accretion luminosity. This long-term variability is scarcely monitored and important questions related to changes in accretion parameters and in accretion modes (such as switching from one-pole to two-pole accretion), as well as to the processes of energy release, are still unanswered.

To properly address some of these issues, a long-term monitoring program of the prototype AM Her was set up with the BeppoSAX satellite in order to investigate its long-term behaviour on a wide (0.1–100 keV) X-ray energy band simultaneously. These observations have been complemented with optical photometry for a more comprehensive study.

2. Observations and data reduction

2.1. The BeppoSAX data

BeppoSAX (Boella et al. 1997) observed AM Her three times, with the source in very different states: a deep low state, an intermediate state, a high state. The journal of the observations is in Table 1. The epochs of the three BeppoSAX observations are also indicated in Fig. 1, superimposed on the secular AAVSO and VSNET optical light curves.

Table 1. Log of BeppoSAX and Optical observations.

Date	MECS Exp. time (s)	Flux ¹ /MECS count rates ²
Sep. 6, 1997	24700	0.085/0.013
May 8, 1998	33500	1.8/0.22
Aug. 12, 1998	80600	12/1.35
Date	Filter	Exp. time (s)
May 20, 1998	No filter	6120
May 21, 1998	No filter	12600
Aug. 20, 1998	V	13320
Aug. 21, 1998	V	10440
Aug. 22, 1998	B	14040
Aug. 23, 1998	U	11880

¹ 2–10 keV, phase averaged flux in units of 10^{-11} erg $\text{cm}^{-2} \text{s}^{-1}$; see de Martino et al. (1998) and the text for best fit models.

² In units of cts s^{-1} .

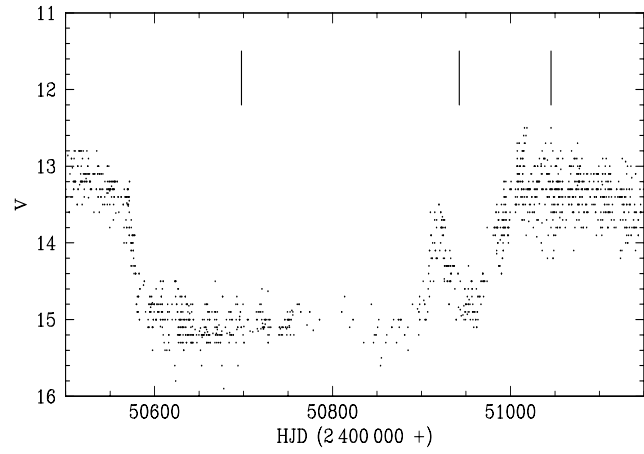


Fig. 1. The secular optical light curve obtained from AAVSO and VSNET showing the three pointings of Sept. 1997, May 1998, and August 1998, corresponding to epochs when AM Her was in a deep low state, an intermediate and high states respectively.

2.1.1. Low state

The source was observed in September 1997 in the midst of a prolonged low state (Fig. 1). During the first four hours the flux level was comparable to that normally observed in low states, when the X-ray emission is still dominated by accretion onto the white dwarf. Then, with a sudden drop by a factor of about 7 in 40 min, the source went into the deepest low state ever observed (see Table 1), in which the X-ray emission was probably at least in part due to coronal emission from the secondary star. Such a fast change in the accretion rate is not easy to accommodate with current scenarios of mass transfer from the secondary and it represents a serious challenge to theoretical models.

The results of this observation have been already published (de Martino et al. 1998), and will not be discussed here any further.

2.1.2. Intermediate state

The second BeppoSAX observation of AM Her was performed in May 1998, after a brief episode of relatively high flux (Fig. 1). In X-rays, the source was at an intermediate flux level, but high enough to permit the temporal and spectral analysis with three BeppoSAX Narrow Field Instruments: LECS (0.1–10 keV), MECS (1.8–10.5 keV) and PDS (15–200 keV). LECS spectra and light curves have been extracted within a 8' radius circular region centred on the source. While for temporal analyses the full LECS band can be used, the spectral analyses have been restricted below 4 keV due to remaining calibration problems at higher energies. The adopted extraction region for the MECS is instead 4'. For both instruments, we have

subtracted the background measured in the same detector regions during blank field observations. In both instruments the source flux is in any case much larger than the background over the whole energy band. For the PDS, which is a collimated instrument, the background is monitored by continuously switching the detectors on and off the source, with a rocking time of 96 seconds, in such a way that 2 out of 4 detectors are always on source. In the following, PDS exposure times refer to the total time during which the source is observed (whatever the pair actually on source), while count rates refer to all 4 detectors.

Net exposure times and time averaged background subtracted count rates are respectively: 16749 s, 0.1273 ± 0.0029 (LECS); 33556 s, 0.2196 ± 0.0026 (MECS, 2 detectors); 30596 s, 0.114 ± 0.068 (PDS). The shorter LECS exposure is due to operational limits on the LECS detector, which can be operated only during satellite nights.

2.1.3. High state

In August 1998, when BeppoSAX observed AM Her for the third time, the source had already recovered its optical high state (Fig. 1). The X-ray flux was also at high level.

Data reduction is as described in the previous subsection. Net exposure times and background subtracted time averaged count rates are respectively: 40053 s, 0.9200 ± 0.0048 (LECS); 80631 s, 1.3510 ± 0.0041 (MECS, 2 detectors); 73214 s, 1.017 ± 0.034 (PDS).

2.2. Optical photometry

AM Her was observed from the Loiano 1.5 m telescope with a 2-channel photoelectric photometer in 1998 May 20 and 21 and August 20, 21, 22 and 23 a few days after the SAX pointed observations. It was at $V \sim 14.5$ mag during May run and white light photometry was acquired with an integration time of 5 s for 1.7 h on May 20 and 3.5 h on May 21. In August it was at $V = 13.51 \pm 0.15$ mag and $B = 13.65 \pm 0.15$ mag. During each night AM Her was observed with an integration time of 1 sec for 3.7 h and for 2.9 h in the V filter on August 20 and 21, respectively; in the band B on August 22 for 3.9 h and in U filter on August 23 for 3.3 h. At irregular intervals of typically 60–120 min sky measures were performed in both channels for about 1 min. Photometric data have been reduced taking into account sky subtraction and differential extinction. Moreover, the V and B data were calibrated using a set of Landolt standards.

3. Temporal analysis

3.1. The X-ray Intermediate State

Both LECS and MECS detectors reveal the typical orbital modulation at $P_{\text{orb}} = 3.09$ hr. Adopting the linear polarization ephemeris quoted in Heise & Verbunt (1988), the

folded light curves in different energy bands are shown in Fig. 2. These are single peaked with a broad maximum (bright phase) centered at $\Phi_{\text{mag}} = 0.6$ and extending between $\phi = 0.4$ –0.8 and with count rates dropping to zero between $\Phi_{\text{mag}} = 0.02$ –0.22 (faint phase). The general shape of the soft and hard X-ray light curves is typical for the intermediate/high state of AM Her, and the BeppoSAX light curves resemble closely those obtained with ASCA in 1993 (Ishida et al. 1997) during a prolonged high state ($V \approx 13.4$). The ASCA light curves are included in Fig. 2 for comparison.

Hence during this epoch AM Her was in its “normal” accretion state, dominated by the primary pole, which is self-occulted during minimum. As in the ASCA or GINGA observations, no significant emission from the secondary pole is observed. Noteworthy is the similarity between the high energy (≥ 0.6 keV) light curve shapes of BeppoSAX and ASCA. An energy dependence of the light curves is also apparent; the curves are more sinusoidal at higher energies (above 4 keV) while more structured at lower energies. Unlike the faint phase count rates, which behave similarly to those at higher energies (i.e. reaching the zero level), the bright phase in the softest range (0.1–0.4 keV) increases between $\Phi_{\text{orb}} \sim 0.5$ –0.7, possibly suggesting a secondary minimum, not covered by the data, at earlier phases. Indeed, the shape of this low-energy LECS light curve departs from the soft X-ray ASCA light curve (0.4–0.6 keV) which in turns compares well with the EUVE light curve of AM Her obtained during a high state, revealing revealing geometric absorption effects in the emission of the main pole (Paerels et al. 1996, Sirk & Howell 1998).

Furthermore, a tendency in the hardness ratios to soften at the rotational minimum is inferred, $[(4\text{--}10\text{ keV}) - (1\text{--}4\text{ keV})]/[(1\text{--}4\text{ keV}) + (4\text{--}10\text{ keV})]$ being -0.29 while it is -0.08 during the bright phase (see also Sect. 3.2 and 4). Also, during the bright phase a significant flickering activity of $\sim 36\%$ with respect to the average is observed in the MECS detector on timescales ranging between 2 mins and 15 mins, while the poor statistics in the LECS detector prevent any detection of rapid fluctuations.

3.2. The X-ray High State

The August 1998 high state light curves, shown in Fig. 3, are characterized by a strong variability. While at energies below 0.4 keV an intense flaring activity is observed, at higher energies the variations are periodic and associated with the white dwarf rotation.

At least 8 flares can be identified in the soft 0.1–0.4 light curve (Fig. 4). The typical duration of these events is longer than the target visibility during one BeppoSAX orbit, preventing the complete coverage of any of the flares. Count rates during these events increase up to a factor of 6 from a mean “quiescence” level of $\sim 0.17 \text{ cts s}^{-1}$. The rise and decay of the better sampled events, as for instance

Table 2. Best fit parameters for the intermediate state, bright phase

#	N_{H}^a (10^{22} cm^{-2})	C^b	kT_{bb} (eV)	kT_{h}^c (keV)	A_Z^d	E.W.^e (eV)	R^f	$\chi^2/\text{d.o.f.} (\chi_r^2)$
1			$19.3^{+3.0}_{-1.4}$	$23.1^{+7.4}_{-4.2}$	$2.77^{+1.10}_{-0.65}$			174/127 (1.37)
2	$2.1^{+1.6}_{-1.1}$	$0.40^{+0.09}_{-0.09}$	$19.6^{+2.7}_{-1.5}$	$13.8^{+4.0}_{-2.6}$	$1.51^{+0.60}_{-0.41}$			143/125 (1.15)
3	$1.35^{+1.45}_{-0.91}$	$0.37^{+0.11}_{-0.11}$	$19.8^{+2.5}_{-1.4}$	$14.4^{+7.1}_{-5.7}$	$1.24^{+0.79}_{-0.65}$	150^{+120}_{-147}	$0.71^{+3.17}_{-0.71}$	135/123 (1.10)

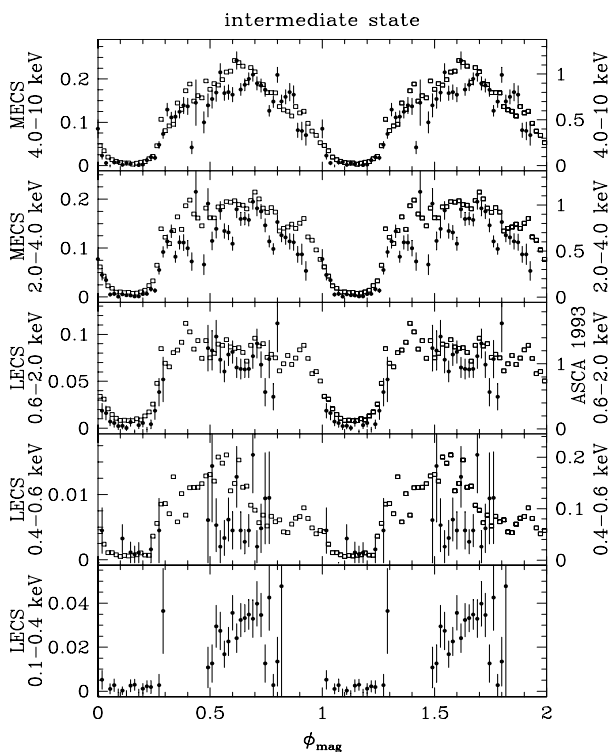
^a Column density of the partial absorber.^b Covering fraction of the partial absorber.^c Plasma temperature.^d Metal abundance in units of the cosmic value (Anders & Grevesse 1989).^e Equivalent width of the 6.4 keV fluorescent iron line.^f Relative normalization of the reflection component (see text).

Fig. 2. LECS (0.1-0.4 keV), (0.4-0.6 keV), (0.6-2.0 keV) and MECS (2-4 keV), (4-10 keV) count rate light curves (black dots) during the intermediate state of May 1998 folded in 55 orbital bins. The intermediate/high state light curves observed by ASCA (open squares) in 1993 are also reported for comparison. Both the BeppoSAX data and the ASCA data are scaled individually to their respective maximum count rates. At this epoch AM Her recovered its “normal” one-pole accretion mode. Note the absence of significant flux during orbital minimum, corresponding to the self-occultation of the primary pole.

the rise of flare f_8 and the decay of flare f_4 have been fitted with an exponential slope resulting in an e -folding time τ of 8 and 22 min, respectively. These events are randomly detected at all magnetic phases and two of them, f_6 and f_7 , indicate that activity is not only related to the main accreting pole. While no hardness ratio can be determined in the narrow 0.1-0.4 keV LECS band, these flares are clearly soft (see also Sect. 4). A soft X-ray flaring behaviour during high states is not uncommon for AM Her (Priedhorsky et al., 1987; Ramsay et al. 1996), but with much shorter time scales (from ~ 30 s to a few minutes). We note, however, that the statistics of LECS data does not allow us to exclude that the observed flares are constituted by train (or series) of shorter events.

In order to inspect the orbital modulation also in the softest channels (≤ 0.4 keV), the eight detected flares have been removed before folding count rates along the magnetic phases.

In Fig. 5 the folded light curves in different bands are shown together with the ASCA ones, all curves again scaled to their respective maximum count rates. The minimum is now significantly above zero at 0.06 cts s^{-1} in the soft (0.1-0.4 keV), at 0.257 cts s^{-1} in the 4-10 keV band and at 0.08 cts s^{-1} in the 13-30 keV band. The BeppoSAX high state light curves are different from any previous X-ray dataset. Particularly remarkable is the lack of orbital modulation in the soft bands (≤ 1 keV), although count rates are slightly lower at $\phi_{\text{mag}} \sim 0.5$ and ~ 0.1 . On the other hand, the hard (≥ 2 keV) X-ray light curves, though still keeping a sinusoidal-like shape as in the intermediate state, have a well defined structured maximum, with a dip occurring at $\phi_{\text{mag}} \sim 0.4$ in the 13-30 keV band, at ~ 0.45 in the 4-10 keV range, and moving to later phases at lower energies. At intermediate energies, in the 1-2 keV range, this dip at $\phi_{\text{mag}} \sim 0.55$ almost reaches the same level as in the primary minimum and mimics a double-humped light curve. The high count rate at orbital min-

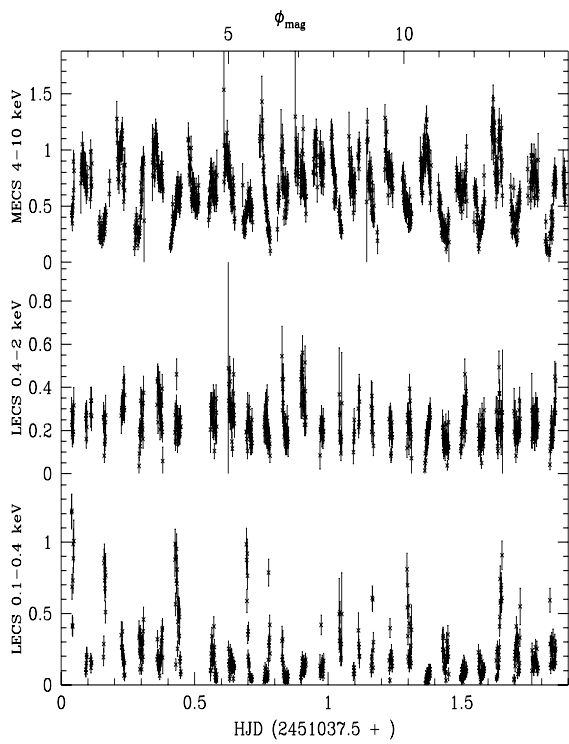


Fig. 3. LECS (0.1-0.4 keV), (0.4-2 keV) and MECS (4-10 keV) 90 sec binned light curves of AM Her during the high state in August 1998 showing a soft flaring activity while the orbital modulation dominates in the hard X-rays.

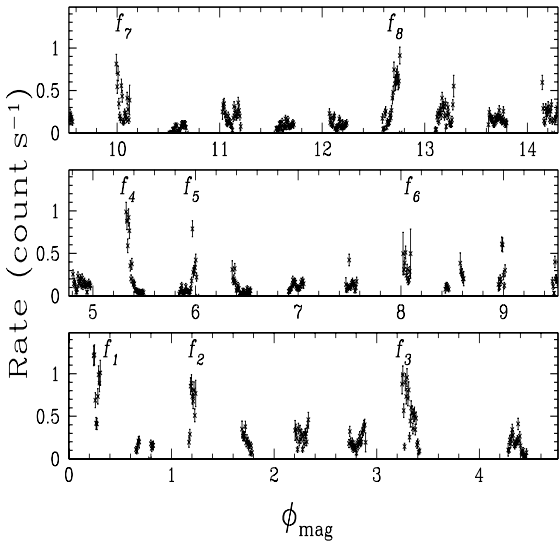


Fig. 4. The LECS (0.1-0.4 keV) 90 sec binned light curve showing strong flaring activity of the order of several tens of minutes.

imum and the modification of the rise and decay shapes of the maximum at high energies suggest a contribution from the secondary pole, which is expected to come into view between $\phi_{\text{mag}} \sim 0.9$ –0.4 (Heise et al. 1985). The lack of a clear soft X-ray modulation indicates that AM Her was not in the so-called “reverse” mode observed by EXOSAT in 1983 (Heise et al. 1985), where the secondary pole was dominating the soft X-ray orbital modulation, but rather in an “atypical” low soft X-ray mode, where the soft X-ray emission from the main pole is comparable to that from the secondary pole. An atypical, but not similar, behaviour was observed in AM Her during a high state in 1976 (Priedhorsky et al. 1987) where no orbital modulation was detected in both soft and hard X-rays. At that epoch the source also showed a soft X-ray flaring activity. The soft X-ray flux was lower by a factor of three than that usually observed during high states. For this uncommon behaviour a shift of the primary pole accretion column and corresponding changes in the absorption pattern were claimed (Priedhorsky et al. 1987). This interpretation however cannot work for the observed behaviour during the 1998 high state, since the lack of orbital modulation is detected only in the soft band. It is hence more likely that the main accreting pole dominates the hard X-ray emission while the secondary pole emission is essentially soft (see also Sect. 4.2). A low soft X-ray emission at all phases could be produced by a decrease in the efficiency of blobby-accretion onto both primary and secondary poles (see also Sect. 5).

At intermediate energies a dip is clearly present in the light curve. An inspection of hardness ratios in different bands reveals a clear hardening at the maximum ($\phi_{\text{mag}} \sim 0.55$), suggesting absorption effects in the accretion column over the main accreting pole.

From Fig. 3, variations on time-scales shorter than the orbital period are apparent. MECS data have been therefore inspected to search for short term variability. The MECS light curve has then been detrended from long-term and orbital variations by subtracting a spline interpolation with a 202 s binning. Then 16 intervals of continuous data with durations between ~ 2200 –3400 s have been selected and for each of them the power spectrum has been computed. The resulting average spectrum of 8 s resolution data, obtained with a uniform rebinning of the individual spectra, is shown in the lower panel of Fig. 6. At high frequencies it goes rapidly to the noise level, corresponding in Fig. 6 to a power of 2, while the low-frequency portion shows a rise at $\nu < 4$ mHz with a shape similar to that inferred from GINGA data by Beardmore & Osborne (1997) and interpreted as shot-noise. Peak features at 1.11 mHz, 1.44 mHz and 2.57 mHz corresponding to 900 s, 694 s and 389 s are also detected at $\sim 3\sigma$ level, and possibly related to flickering produced by inhomogeneities in the accretion flow.

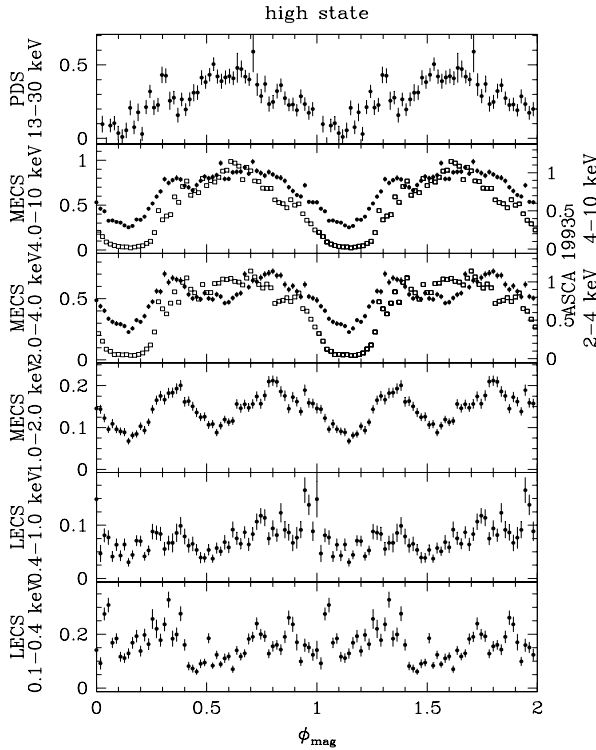


Fig. 5. High state LECS (0.1-0.4 keV), (0.4-1 keV), MECS (1-2 keV), (2-4 keV), (4-10 keV) and PDS (13-30 keV) folded light curves (black dots) compared to the same ASCA data (ordinates are scaled to the maximum). Flares observed in the softer band have been removed before folding. Contrary to the intermediate states of May and ASCA these light curves reveal a significant emission during the faint phase. A dip feature around $\phi \sim 0.45$ (at high energies) increasing in depth and moving towards later phases at lower energies is also observed.

3.3. The optical variability

Intermediate state white light photometry reveals weak (~ 0.18 mag) orbital modulation but strong ($\gtrsim 0.4$ -0.5 mag) flaring-type cycle-to-cycle variability which, together with the short duration of the observations, only allows one to identify a maximum around $\phi_{\text{mag}} \sim 0.8$. The flare durations range between a few mins to a few tens of minutes.

Differently, the high state V band light curve shows a strong orbital behaviour, whilst U and B photometry have a less pronounced variability (Fig. 7). In the V band the light curve is strongly non-sinusoidal with a well defined broad primary minimum ranging between $\phi_{\text{mag}} \sim 0.4$ -0.7 and a flat-topped maximum; a secondary minimum centered at $\phi_{\text{mag}} \sim 0.1$ is also apparent. Such shape of the V band modulation and the presence of a secondary minimum are known to be characteristic of AM Her during high states (Mazeh et al. 1986 and reference therein; Wickramasinghe et al. 1991; Beardmore & Osborne 1997). Exception is the peculiar behaviour observed in 1976, when AM Her was lacking a clear orbital X-ray modulation and

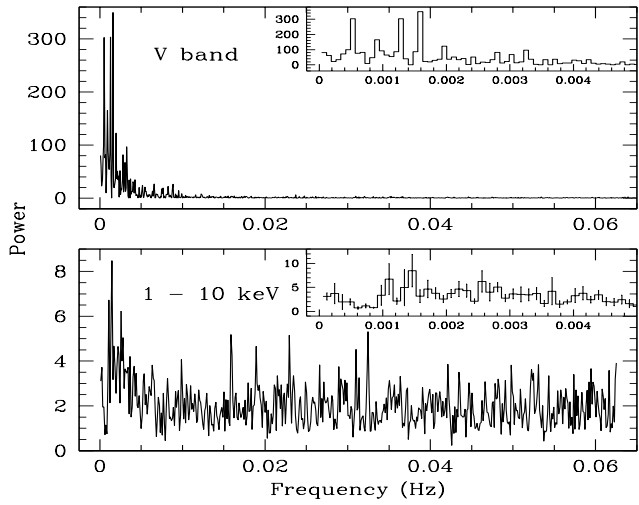


Fig. 6. The average power spectra in the high state of 5 s resolution time V filter data (upper panel) and of 8 sec time resolution MECS data (lower panel). The normalization adopted is such that the white noise level corresponds to a power of 2. The inserted enlargements show the presence of peak features discussed in the text.

when the optical secondary minimum disappeared (Priedhorsky et al. 1987). On the other hand, the U and B band light curves are different, though the primary minimum around $\phi_{\text{mag}} \sim 0.5$ is still observed and the secondary minimum can be possibly recognized in the B filter despite of the presence of short-term variability (see below). Noteworthy is that in the U band the shape is sinusoidal-like with a maximum around $\phi_{\text{mag}} \sim 0.9$. This is consistent with what observed in May in white light and during other intermediate states (Beardmore & Osborne 1997). However, there is a marked difference with respect to low state optical observations (Bonnet-Bidaud et al. 2000), where the light curves, especially in the U and B bands show similar phasing to that observed in the UV during low states, with a maximum at $\phi_{\text{mag}} = 0.6$, where the main accreting pole dominates (Gänsicke et al. 1995). Hence all this is in favour of a strong cyclotron beaming in the V band and a substantial contribution from the secondary pole at shorter wavelengths. A detailed modeling of the V band orbital modulation with cyclotron emission is the subject of a forthcoming paper (Gänsicke et al. in preparation).

A marked flickering type variability is also observed in the optical data with typical amplitudes of 0.1-0.5 mag. The time-scale of this activity (a few minutes) is different from that observed in the soft X-rays. In order to inspect these variations the long-term and orbital trends have been removed by subtracting a cubic spline interpolation of a large binning of the data. Data centered on the optical maximum and minimum have been selected, and

for each of them the power spectrum has been computed. The average power spectrum (upper panel of Fig. 6) indeed shows not only a low frequency rise at $\nu \leq 2$ mHz but also peak features, at 0.5 mHz, 1.3 mHz and 1.6 mHz, corresponding to 2000 s, 769 s and 625 s at $\sim 5\sigma$ level. These variations are consistent with those inferred in hard X-rays, suggesting that they are related to the post shock accreting region.

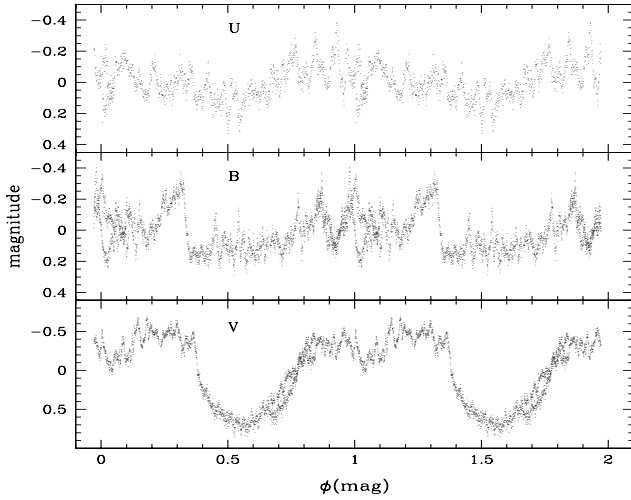


Fig. 7. High state U B V light curves of August 1998, binned in 10 s (U) and 5 s (B, V) intervals, showing a marked difference between V band and U and B filters. A pronounced minimum at $\phi \sim 0.55$ is a common feature, while a secondary minimum is clearly detected in the V light curve at $\phi \sim 0.1$ but somewhat corrupted by short-term flaring type variability in the other bands (see text).

4. Spectral analysis

4.1. Intermediate state

The flux level of the source in this observation is not sufficient to allow a detailed phase-resolved spectroscopy. The flux is virtually zero at the minimum phase, and in order to increase the signal-to-noise the spectrum has been selected over the bright phase between $\phi_{\text{mag}}=0.4$ and 0.8. The results are summarized in Table 2. (Hereinafter, the relative normalization between LECS and MECS has been left free to vary to allow for the different time coverage, while that between PDS and MECS has been kept fixed to 0.84). Firstly, we introduced only the very basic spectral components for a polar: a black body, and an optically thin thermal plasma emission (model MEKAL in the spectral package XSPEC). The galactic absorption has been fixed to the value of $9 \times 10^{19} \text{ cm}^{-2}$ (Gänsicke et al. 1995). The fit is poor ($\chi^2_{\nu}=1.37$), and the iron abundance is quite large (2.8). Inspection of the residuals (Fig. 8) suggests the

presence of complex absorption. The addition of a partial absorber improves significantly the quality of the fit; the plasma temperature diminishes considerably, and so does the iron abundance. A further improvement in the fit quality (and a decrease of both the temperature and the iron abundance) is achieved by adding a neutral iron line at 6.4 keV, as suggested by small residuals around that energy and by analogy with previous GINGA and ASCA observations (Beardmore & Osborne 1997; Ishida et al. 1997) and with the high state data described below. A Compton reflection continuum (Matt 1999 and references therein), which is expected to be present along with the neutral iron line, has also been included, even if not required by the data. The improvement in the quality of the fit is significant at the 97% confidence level (F-test). The value of R in Table 2 represents the solid angle subtended by the cold matter in units of 2π , assuming a viewing angle of 60° .

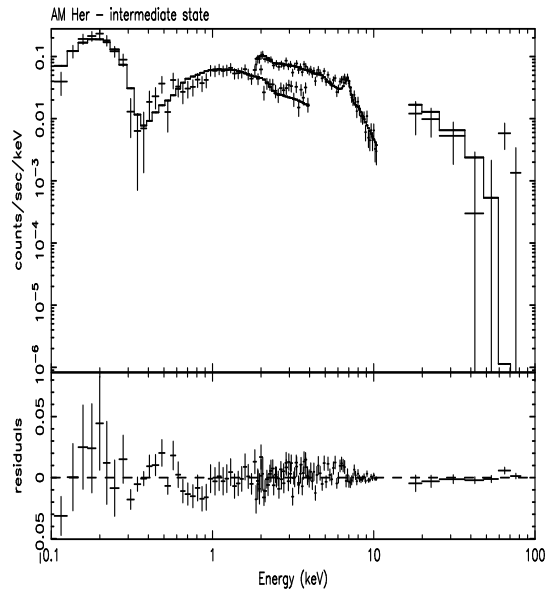


Fig. 8. Data and residuals for the intermediate state, bright phase, when fitted without partial absorption, the neutral iron line and the Compton Reflection continuum.

4.2. High state

The much better statistics for the high state (due to both a higher flux and a longer exposure time), together with the fact that in this state there is significant emission also during the minimum, permits to perform a phase-resolved spectroscopic analysis. The bright phase ($\phi=0.4-0.9$) spec-

trum has been constructed excluding the data during the flares discussed above. The results are reported in Table 3, where the same sequence of models have been applied. The simplest model (black body plus thermal plasma emission) is now completely unacceptable. The inclusion of partial absorption provides a dramatic improvement in the fit, which however is still unacceptable. The neutral iron line and the Compton reflection continuum are both required by the data (see Fig. 9). If only the line is included, the χ^2 is 144 for 127 d.o.f; apart from physical considerations, the reflection continuum is required at the 99.7% confidence level, according to the F-test.

Instead, a multi-temperature plasma and/or ionized or more complex absorption do not improve the statistical quality of the fit.

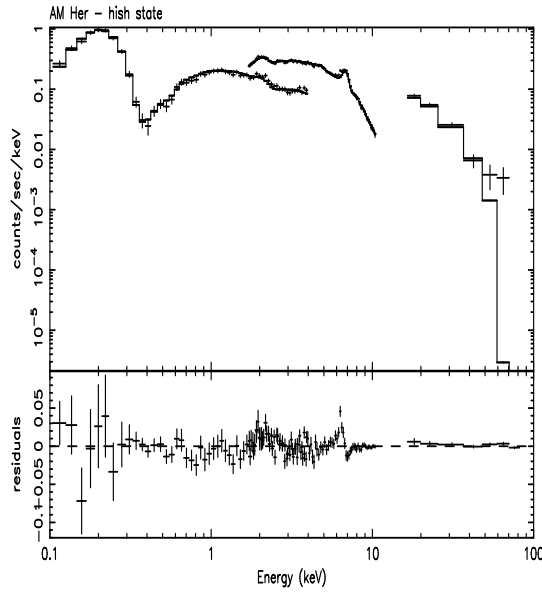


Fig. 9. Data and residuals for the high state, bright phase, when fitted without the neutral iron line and the Compton reflection continuum.

The folded light curve has then been divided in 10 phase bins, and the LECS+MECS spectra have been analysed for each bin. Again, flares were excluded. The adopted model is the same as before, except for the reflection component which is an unnecessary complication at this level of statistics. The iron abundance was fixed at the best fit value for the bright phase, i.e. 0.89 times the solar value. In Fig. 10 the blackbody and plasma temperatures are shown as a function of phase. Both temperatures are consistent with being constant. Fixing them to their bright phase best fit values (model 3 of Table 3), we derived the

bolometric luminosities of the two spectral components, which are shown in Fig. 11 along with their ratio. It is worth noting that the fluxes are corrected for absorption, and then any variation should be intrinsic. At the minimum the spectrum is significantly softer than at the maximum (as also discussed in sect. 3.2 where, however, effects of absorption were not separated). As the blackbody temperature is constant, the increase of the soft emission is due to an increase of the emitting area. The simplest explanation is that the secondary pole is active. Furthermore, the fact that a similar increase is not present in the hard component suggests that, at the secondary pole, accretion mainly occurs in the form of high density blobs, shocking deep in the photosphere.

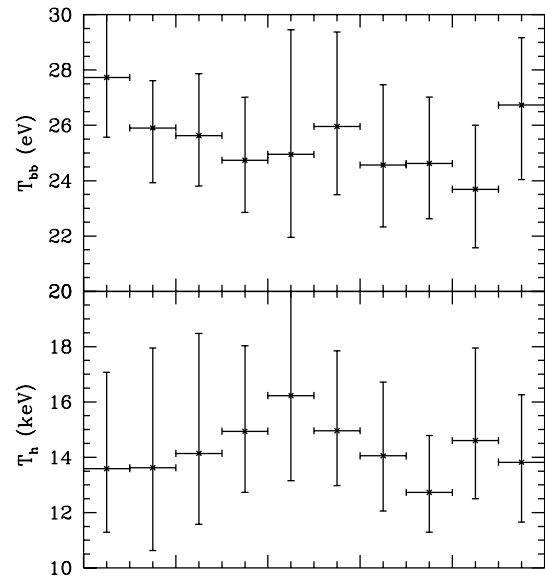


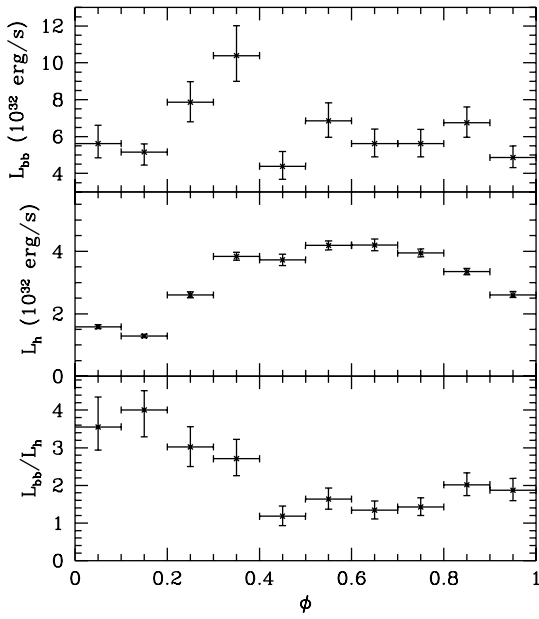
Fig. 10. Black body (upper panel) and thermal plasma (lower panel) best fit temperatures as a function of the orbital phase.

A search for any phase-dependence of the partial absorption (Fig. 12) has also been performed. The column density (upper panel) of the absorber has a maximum around $\phi_{\text{mag}}=0.4-0.7$, while the covering factor (middle panel) increases steadily up to around $\phi_{\text{mag}}=0.5-0.6$, and then decreases. This is not surprising, because at this phase the angle between the line of sight and the accretion column is minimum, and then the amount of cold matter along the line of sight is likely to be the largest.

In the lower panel of Fig. 12, the equivalent width (EW) of the iron K α 6.4 keV line is plotted. The ϕ -dependence of this parameter is what expected if the line

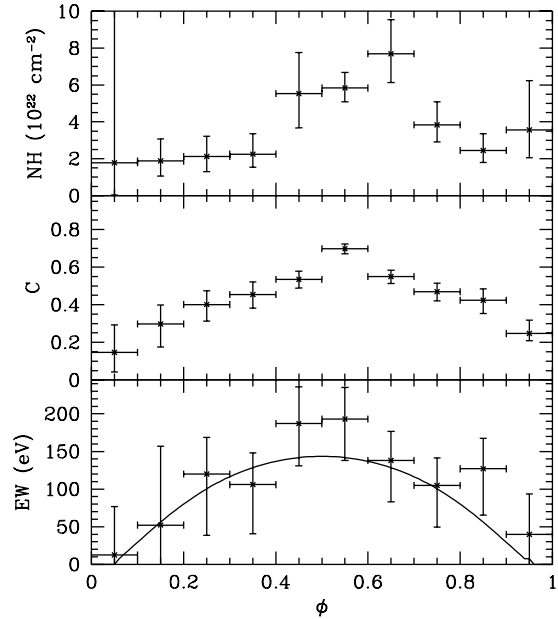
Table 3. Best fit parameters for the high state bright phase.

#	N_H (10^{22} cm^{-2})	C	kT_{bb} (eV)	kT_h (keV)	A_Z	E.W. (eV)	R	$\chi^2/\text{d.o.f. } (\chi^2_r)$
1			$24.7^{+1.1}_{-1.2}$	$32.7^{+2.0}_{-1.7}$	$5.09^{+0.49}_{-0.44}$			1504/130 (11.6)
2	$4.97^{+0.69}_{-0.59}$	$0.51^{+0.2}_{-0.2}$	$24.7^{+1.2}_{-1.1}$	$16.9^{+0.9}_{-0.8}$	$1.38^{+0.15}_{-0.14}$			255/128 (1.99)
3	$3.56^{+0.57}_{-0.49}$	$0.50^{+0.02}_{-0.02}$	$25.0^{+1.1}_{-1.2}$	$13.7^{+2.2}_{-1.4}$	$0.89^{+0.21}_{-0.14}$	107^{+37}_{-26}	$1.43^{+0.75}_{-0.74}$	134/126 (1.07)

**Fig. 11.** Black body (upper panel) and thermal plasma (middle panel) luminosities ($D=91$ pc), and their ratio (lower panel), as a function of the orbital phase.

is originated in the white dwarf photosphere illuminated by the hard X-ray radiation emitted by the post-shock region. In fact, because the photosphere is optically thick, the line EW has a well known angular behaviour (Matt et al. 1991; George & Fabian 1991; see also Matt 1999), decreasing with the viewing angle. This is shown in the figure, where the expected line EW (calculated following Basko 1978 and assuming: a plane parallel geometry; a 13.7 keV bremsstrahlung illuminating spectrum; and an iron abundance of 0.89 times the solar value, see Table 3) is also plotted (solid curve), adopting the inclination and colatitude of the primary pole as given by Cropper (1988).

Finally, the spectrum during flares has been analysed, summing data from all flares. The spectrum is significantly softer than during quiescence, whatever the phase. For an assumed distance of 91 pc (Gänsicke et al. 1995), the blackbody luminosity is in fact $12.4^{(+2.7)}_{(-1.9)} \times 10^{32}$ erg s $^{-1}$, while that of the hard emission is $2.29^{(+0.16)}_{(-0.12)} \times 10^{32}$ erg s $^{-1}$, the ratio being then ~ 5.4 . While the parameters of the hard emission are substantially the same, the blackbody temperature is somewhat higher, $30.4^{(+1.3)}_{(-1.1)}$ eV. Similar values for the flare and “quiescence” temperatures were found from ROSAT data (Ramsay et al. 1996).

**Fig. 12.** Column density (upper panel) and covering factor (middle panel) of the partial absorber, and the EW of the neutral iron line (lower panel), as a function of the orbital phase. In the lower panel, the expected values of the line EW are also shown (solid curve; see text for details).

5. Discussion and conclusions

The BeppoSAX data presented here have shed new light onto the temporal and spectral behaviour of AM Her.

The observations carried out at different brightness levels indicate that the accretion mode can be substantially different. During intermediate states, accretion occurs mainly in the “normal” mode, with the primary pole dominating both hard and soft X-ray emissions. A 20 eV soft black body and a 14 keV temperature for the thermal plasma are found, provided the inclusion of partial absorption, of a reflection component and of an iron K α 6.4 keV line with EW = 150 eV.

High states instead can be very different from epoch to epoch. Differently from previous observations, our BeppoSAX high state observation shows a markedly different variability in the soft and hard X-rays. A strong flaring activity characterized by an increase in flux by a factor of 5–10 with typical exponential rise and decay time-scales of the order of tens of minutes is observed below 0.4 keV. In hard X-rays the variability is essentially related to the orbital modulation. Differently from intermediate and previous high state observations, the presence of significant emission during the faint phase in both soft and hard X-rays provide evidence that the secondary pole is emitting. Furthermore, the lack of an orbital variability in the soft X-ray “quiescence” emission contrasts with the strong modulation observed in hard X-rays. This suggests that soft X-ray emission from the primary pole (whatever produced by blobs or by reprocessing of hard X-rays) is highly inefficient. An atypical low soft X-ray emission period was indeed observed in the past in AM Her during a high state (Priedhorsky et al. 1987) but accompanied by the lack of the X-ray minimum in both soft and hard bands. While this was interpreted by a shift in the accretion column with a corresponding change of the accretion pattern, the behaviour observed in August 1998 appears to be better explained by the onset of accretion onto the secondary pole whose emission is mainly soft together with a less active soft X-ray production from the primary pole.

It is worth noting that the soft flaring activity appears to be related to both accreting poles. The observed flaring activity is not uncommon for AM Her but with much shorter time scales. Furthermore similar variations are not observed in the UVW coordinated photometry indicating that the soft X-ray flares are unrelated to the optical cyclotron post-shock emission. Moreover, spectral analysis of flares indicates a higher temperature of the soft black body (~ 30 eV) while the hard X-ray emission has not varied.

The August high state BeppoSAX data have also revealed for the first time a strong energy dependence of the orbital modulation which moves from a single-humped shape at high energies (4–30 keV) to a double-humped shape around 1 keV. This effect can be explained in terms

of absorption in the accretion column when pointing towards the observer.

For this high state, it has been possible to perform a phase-resolved spectral analysis, and to measure the parameters of both black body and optically thin thermal plasma emission along the orbital phase. The temperatures of both components are consistent with being constant, and compatible with those inferred for the May intermediate state. The plasma temperature (14 keV) also agrees with the ASCA data, but not so the black body temperature, which is 25 ± 1 eV (ASCA: 32 ± 1 eV). The latter is however in agreement with EUVE (24.5 eV) (Ishida et al. 1997). The phase dependence of the partial absorber is indeed compatible with an increase of the amount of cold matter when the accretion column is along the line of sight. The dip observed at $\phi_{mag} \sim 0.5$ is consistent with such an increase, as both covering fraction and column density are higher. The phase dependence of the EW of the neutral iron line is consistent with an origin in the white dwarf surface illuminated by the hard X-rays from the post-shock regions.

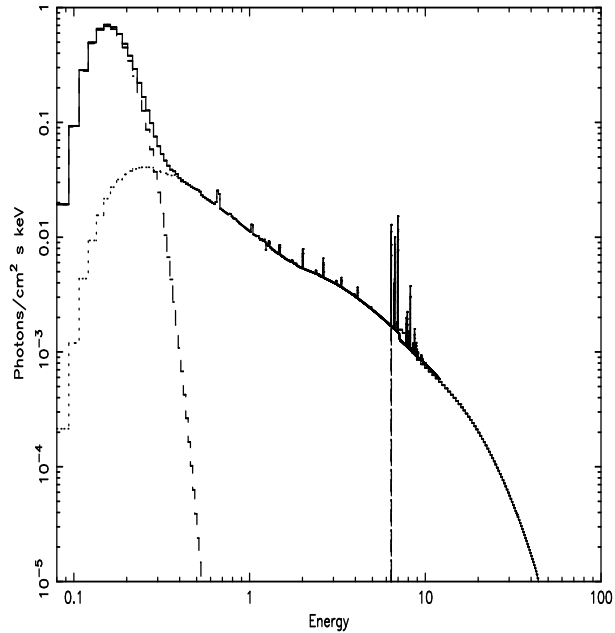


Fig. 13. Best fit model for the high state, bright phase (model 3 in Table 3).

Fixing the black body temperature of both intermediate and high states to 25 eV and that of the optically thin thermal plasma to 14 keV, the bolometric luminosities of these components at the maximum, and adopting $D = 91$ pc, are: $L_{BB} = 0.81^{(+0.31)}_{(-0.17)} \times 10^{32} \text{ erg s}^{-1}$ and $L_{Th.} = (0.683^{+0.027}) \times 10^{32} \text{ erg s}^{-1}$ for the intermediate state;

whilst for the high state these are $L_{BB} = (5.32^{+0.31}_{-0.60}) \times 10^{32} \text{ erg s}^{-1}$ and $L_{Th.} = (3.333^{+0.047}_{-0.037}) \times 10^{32} \text{ erg s}^{-1}$. We note that while the hard X-ray luminosities are typical of intermediate and high states, that of the black body component during the high state is lower than previously measured. This is shown in Fig. 13, which can be compared with that reported by Ishida et al. (1997) for the intermediate state in 1993. The inferred soft-to-hard X-ray ratio is 1.2 and 1.6 during the intermediate and high state, respectively. It has been shown that in AM Her the bulk of reprocessed hard X-ray and cyclotron radiations emerges in the UV range rather than in the soft X-rays (Gänsicke et al. 1995), the latter being mainly produced by the blobby accretion mechanism. During the high state observed in August, both the inferred black body luminosity and the lack of a clear modulation in the soft X-ray band suggest that discrete accretion onto the primary pole is not as efficient as in other epochs. Given the low level of soft X-ray flux during the faint phase it is not possible to infer the black body luminosity from the secondary pole. From the high state black body luminosity during the bright phase, information on the mass accretion rate can be estimated. A value of $8.5 \times 10^{-11} M_{\odot} \text{ yr}^{-1}$ for a white dwarf mass of $0.6 M_{\odot}$ is derived. A fractional accreting area $f \sim 2.4 \times 10^{-4}$ is obtained, which is a factor of $\sim 3\text{-}10$ larger than those derived by Gänsicke et al. (1995) and Ishida et al. (1997) respectively during typical high states. The local mass accretion rate then results to be $\sim 4 \text{ g s}^{-1} \text{ cm}^{-2}$ which is too low to make blobby accretion efficient.

As far as flares are concerned, the changes are essentially related to an increase in the temperature of the soft component, as also observed during other flaring epochs (Ramsay et al. 1996). The increase in black body luminosity and then in the mass accretion rate is a factor of 2 with respect to “quiescence”, and comparable to usual high state values. Our estimates of the fractional area of the emitting black body during flares results to be similar to that during “quiescence” which gives a low local mass accretion rate of $\sim 8 \text{ g s}^{-1} \text{ cm}^{-2}$. However, since we cannot exclude that accretion occurs onto a more localized area, we consider this value as a lower limit.

Different from the flaring variability are the rapid fluctuations detected in the hard X-rays and optical ranges, the latter likely to be associated with inhomogeneities in the accretion flow itself.

Furthermore, the optical orbital modulation observed in August is typical of AM Her during high states, where the V band is dominated by cyclotron beaming from the primary pole (Gänsicke et al. in preparation). The secondary pole instead appears to dominate at optical blue wavelengths. This is very different from low and other high states where the main accreting pole usually dominates the UV and the blue portion of the optical spectrum.

In summary, the present observations reveal that AM Her has switched from a “normal” accretion mode during the intermediate state of May 1998 into a “two-pole” accretion mode during the high state of August 1998, with a less efficient “blobby” accretion onto the primary pole.

Acknowledgements. We acknowledge the BeppoSAX SDC team (and in particular Paolo Giommi, Fabrizio Fiore and Angela Malizia) for providing pre-processed event files and for their constant support in data reduction and analysis. We thank the BeppoSAX mission scientist, Luigi Piro, for his intelligent handling of the schedule, and the mission planning team (Donatella Ricci, Milvia Capalbi and Sonia Rebecchi) for the courtesy and patience. The timely observations of the source in different states would not have been possible without the informations provided by AAVSO: we warmly thank dr. J. Mattei and the entire AAVSO team. We thanks Lucio Chiappetti for useful comments on an early version of the manuscript. GM and DdM acknowledge financial support from ASI.

References

Anders E., Grevesse N., 1989, Geochim. and Cosmochim. Acta 53, 197
 Basko M.M., 1978, ApJ 223, 268
 Beardmore A.P., Osborne J.P., 1997, MNRAS 290, 145
 Beuermann K., 1998, in *Perspectives in High Energy Astronomy and Astrophysics*, P.C. Agrawal and P.R. Visvanathan eds., India Univ. Press, p. 100.
 Boella G., Butler R.C., Perola G.C., et al., 1997, A&AS 112, 299
 Bonnet-Bidaud J.M., Mouchet M., Shakhovskoy N.M., et al., 2000, A&A in press
 Cropper M., 1988, MNRAS 231, 597
 Cropper M., 1990, Space Science Rev. 54, 195
 Cropper M., Ramsay G., Wu K., 1998, MNRAS 293, 222
 de Martino D., Gänsicke B.T., Matt G., et al., 1998, A&A 333, L31
 Gänsicke B.T., Beuermann K., de Martino D. 1995, A&A 303 127
 George I.M., Fabian A.C., 1991, MNRAS 249, 352
 Heise J., Verbunt F., 1988, A&A 189, 112
 Heise J., Brinkman A.C., Gronenschild E., 1985, A&A 148, L14
 Ishida M., Matsuzaki K., Fujimoto R., Mukai K., Osborne J.P., 1997, MNRAS 287, 651
 Kuipers J., Pringle J.E. 1982, A&A 114, L4
 Lamb D.Q., Masters A.R. 1979, ApJ 234, L117
 Matt G., 1999, Annapolis Workshop on Magnetic Cataclysmic Variables, ASP Conference Series, Volume 157, edited by Coel Hellier and Koji Mukai, p. 299
 Matt G., Perola G.C., Piro L., 1991, A&A 245, 25
 Mazeh T., Kieboom K., Heise J., 1986, MNRAS 221, 513
 Paerels F., Hur M.Y., Mauche C.W., Heise J., 1996, ApJ 464, 884
 Priedhorsky W., Marshall F.J., Hearn D.R., 1987, A&A 173, 95
 Ramsay G., Cropper M., Mason K.O., 1996, MNRAS 278, 285
 Sirk M.M., Howell S.B., 1998, ApJ 506, 824
 van Teeseling A., Heise J., Paerels F., 1994, A&A 281, 119

Wickramasinghe D.T., Bailey J., Meggett S.M.A., 1991, MN-
RAS 251, 28